Along-Strike Geochemical Variations in the Late Triassic Nikolai Magmatic System, Wrangellia, Central Alaska

Alicja **WYPYCH**[1] (alicja.wypych@alaska.gov), Evan **Twelker**[1], Lauren **Lande**[1,2], Rainer **Newberry**[2]
[1]Alaska Division of Geological & Geophysical Surveys, [2]University of Alaska Fairbanks

INTRODUCTION

The Triassic Nikolai Basalt and related mafic to ultramafic intrusions are one of the world's most complete and best exposed sections of a large igneous province (Amphitheater Mountains, Alaska), and have been explored for magmatic Ni-Cu-Co-PGE mineralization (Wellgreen deposit, Kluane Ranges, Yukon Territory, and Eureka zone, Eastern Alaska Range, Alaska). The full extent of the basalts and intrusions, as well as magma generation processes are yet to be fully established. Two hypotheses have been put forward to explain the geochemical variation in Nikolai Basalts: 1) a deep mantle plume (Greene et al., 2008), and 2) decompressional melting of mantle beneath a back-arc/intra-arc spreading center (Taylor et al., 2008). To better understand the extent and magmatic architecture of the Nikolai system, investigate the mineral potential and explore the two hypotheses of basalt generation, the Alaska Division of Geological & Geophysical Surveys (DGGS) conducted mapping and geochemical investigations of the province from 2013 through 2015.

We present major and trace element data from whole rocks and olivine from Triassic basalts and intrusive rocks collected over a 250 km along-strike transect. Chemical compositions of whole rock samples were obtained using inductively coupled plasma atomic emission spectroscopy and inductively coupled plasma mass spectrometry. This data is used to answer questions about variations in magma generation, temperature of crystallization, and degree of fractional crystallization required to produce the Nikolai Basalts.

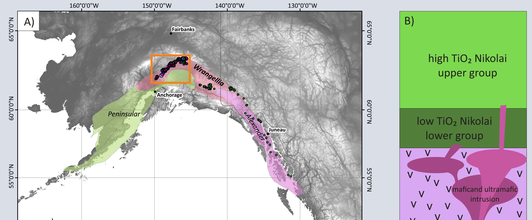

Fig. 1. A) Geographic distribution of Triassic mafic and ultramafic rocks (green dots represent data collected by Taylor et al. [2008], Greene et al. [2008, 2009]), the blue, pink and maroon dots represent samples collected by DGGS during 2013-2015 field seasons (Twelker et al., 2014; Wypych et al., 2014; Wypych et al., 2015). Pink, red and green shaded polygons represent Alexander, Wrangellia and Peninsular Terranes (USGS data), the orange rectangle outlines the area of focus of this study. The Nikolai Basalts in the region of interest erupted onto the Skolai Arc (Nokleberg et al., 1994).
B) Schematic cross section through Paleozoic and Triassic metavolcanic and metasedimentary rocks in the study area. Skolai Arc in the region is build mostly with andesitic metavolcaniclastic rocks with some rhyolitic layers, and is capped by limestone and marble. Overlying low TiO_2 Nikolai (Late Triassic) and High TiO_2 Nikolai are largely metabasalts and meta-basaltic andesites. The mafic and ultramafic intrusions (low and high TiO_2) are interpreted as feeders to the Nikolai basalts.

GEOCHEMISTRY OF THE TRIASSIC MAFIC AND ULTRAMAFIC ROCKS

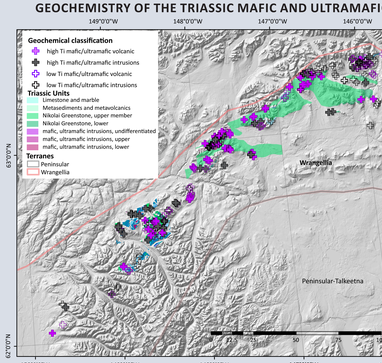

Fig. 2 Rock samples classified based on titanium and zirconium composition (Pearce and Cann, 1973). High TiO_2 volcanic rocks lie stratigraphically on top of low TiO_2 volcanicrocks, and generally have greater thickness (Twelker et al., 2015), however the geographic distribution of both is similar.

GEOCHEMISTRY OF TRIASSIC MAFIC AND ULTRAMAFIC ROCKS

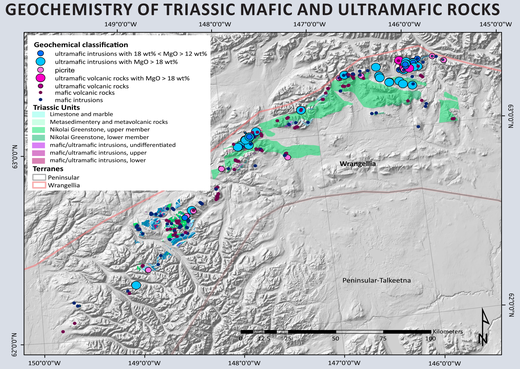

Fig. 3. Geographic distribution of geochemically differentiated rocks in the map area. The geochemical classification of mafic and ultramafic rocks is based on silica, potassium, sodium and magnesium oxide composition (LeBas et al., 1986; 2000). The larger the circle, the more magnesium rich the rock. The high and very high Mg rocks tend to concentrate in the NE corner of the map area, and dissipate towards the SW.

GEOCHEMICAL CLASSIFICATION OF MAFIC VOLCANIC AND PLUTONIC ROCKS

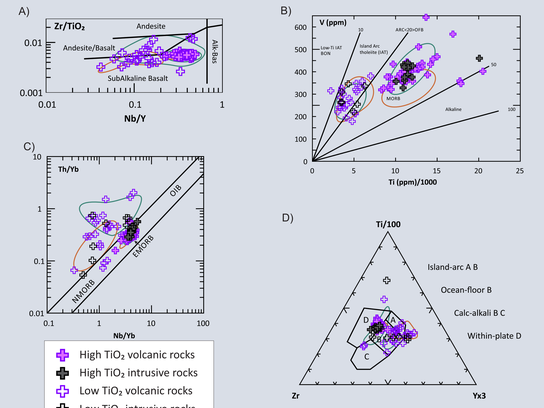

Fig. 4. A) Winchester and Floyd (1977) geochemical classification of Nikolai volcanic rocks. Two groups (open and closed symbols) represent low- and high-TiO_2 composition of the basalts (lower and upper group). Lower group basalts tend to plot within the basalt to subalkaline basalt field, whereas upper group basalts plot solely in the subalkaline basalt field. The upper and lower groups are also distinguished by their V and Zr composition; the upper group plot within MORB fields both on the Shervais (1982) diagram (fig. B), and Pearce and Cann (1973; Ti vs. Zr plot, not shown), and the lower group plot mostly within Island Arc Tholeiites.
C) On Pearce`s (2008) diagram, samples from the upper group plot tightly within enriched MORB field, whereas the lower group samples scatter mostly above the MORB array suggesting additional processes involved in the formation of those rocks.
D) Zr-Ti-Y diagram (Pearce and Cann, 1973) shows samples from upper group displaying within-plate classification, and the lower group scatter mostly towards island-arc/ocean floor fields.

Green polygons outline upper and lower Nikolai basalts analyzed by Taylor et al. (2008) and orange polygons outline data collected by Greene et al. (2005; 2008; 2009). DGGS data geerally falls within their compositional polygons.

PRELIMINARY MAJOR AND TRACE ELEMENT MODELING

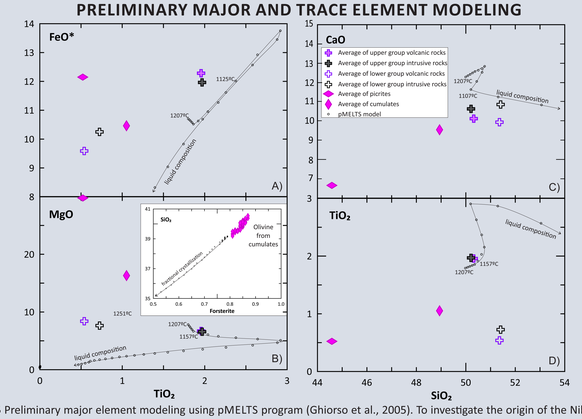

Fig. 5 Preliminary major element modeling using pMELTS program (Ghiorso et al., 2005). To investigate the origin of the Nikolai magmas we undertook pMELTS modeling; here we show experiments conducted at 500 bars pressure, with starting temperature of 1200º C and 50º C steps. Since the high TiO_2 group of Nikolai basalts and intrusions plot in the EMORB field (fig. 4 B, and C) we used EMORB composition as a starting point (compositions from Waters et al., 2010). We find that the high TiO_2 group can easily be explained by simple partial mantle melting followed by about 10 to 20% fractional crystallization, however this mantle composition is not capable of producing the low TiO_2 group Nikolai Basalt. The diamonds tend to plot as more mafic than the volcanic and intrusive "normal groups". They have been flagged as different because of their very high MgO content, and are interpreted by us as cumulates from the fractional crystallization of the Nikolai magma. The major element fractional crystallization patterns seem to support this interpretation (especially diagrams B and D). To further investigate the theory that the very high MgO samples are in fact cumulates, we performed a similar MELTS experiment using the most mafic basalt composition both for high TiO_2 and low TiO_2 group Nikolai as starting liquid composition (insert into diagram 5 B) and plotting olivine composition crystallizing from that liquid composition against olivine composition measured by electron microprobe with wavelength dispersive X-ray spectroscopy. Olivines from the cumulates always plot as more mafic than the high TiO_2 Nikolai group and fall along the sample fractional crystallization trend, but cannot be explained by fractional crystallization of the low TiO_2 group.

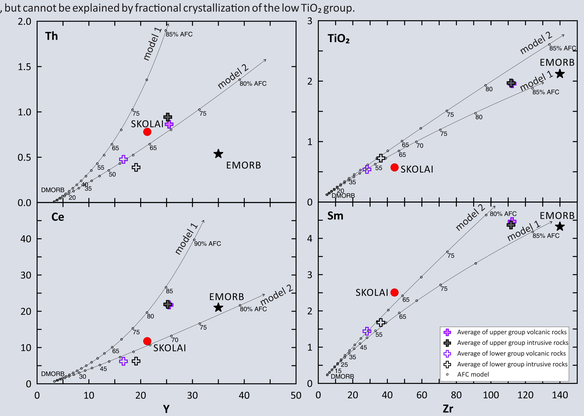

Fig. 6 Assimilation - Fractional Crystallization (AFC) Models (DePaolo, 1981). Since normal EMORB melting and fractional crystallization cannot explain the low TiO_2 Nikolai group we conducted trace-element modeling. The models presented here are the best fit to explain our data. Both models were run with depleted MORB (DMORB; Workman and Hart, 2005) as parental magma and average composition of Skolai Arc (red circle; Wypych et al., 2014) as assimilant, with a fractional crystallization to assimilation ratio of 3.28 and at 1 atm pressure. In model 1 we used 20% olivine, 65% of clinopyroxene and 15% feldspar as fractional crystallization material and in model 2 we crystallized 65% olivine, 20% clinopyroxene and 15% feldspar - both the compositions are present within the most mafic intrusions in the region. Other experiments (simple fractionation of MORB, EMORB, DMORB, and AFC of EMORB and Skolai Arc) have been conducted, however none of those was able to simulate the chemical composition of the Nikolai groups. The models are plotted on bivariate plots (Th vs. Y, Ce vs. Y, TiO_2 vs. Zr and Sm vs. Zr) with average low TiO_2 and high TiO_2 groups and cumulates. 50 to 60 % of assimilation and fractional crystallization of the experiment with crystallization of 65% olivine, 20% of clinopyroxene and 15% of feldspar best explain the low TiO_2 Nikolai composition. The high TiO_2 Nikolai group can be explained by both experiments, however model 1 is a slightly better fit.

PLATINIUM GROUP PROVENANCING

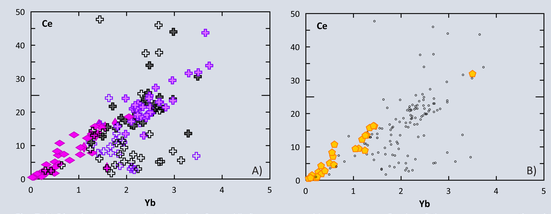

Fig. 7 A) Bivariate scatter plot showing Ce vs. Yb for upper and lower groups. Rocks of the upper magmatic suite plot along a positively sloped trend with higher Ce:Yb ratios, reflecting their characteristic enriched REE pattern. The rocks of the lower suite generally have lower Ce:Yb ratio, and scatter similarly to fig.4. Olivine cumulates have low total REE values because REE are incompatible in olivine; nevertheless, many of the cumulate rocks retain the Ce:Yb ratio of the high TiO_2 magmatic suite. B) The same plot showing samples with elevated values of Pt and Pd. These data indicate that PGE mineralization occurs in cumulate rocks associated with upper Nikolai group magmas.

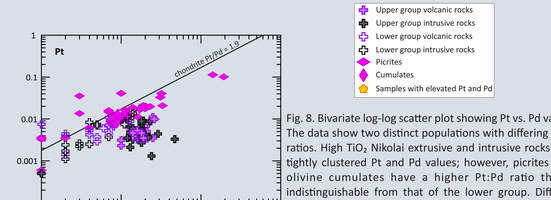

Fig. 8. Bivariate log-log scatter plot showing Pt vs. Pd values. The data show two distinct populations with differing Pt:Pd ratios. High TiO_2 Nikolai extrusive and intrusive rocks have tightly clustered Pt and Pd values; however, picrites and olivine cumulates have a higher Pt:Pd ratio that is indistinguishable from that of the lower group. Differing characteristic Pt:Pd ratios may reflect the conditions of mantle melting or magma ascent.

Maier and Barnes (2004) ascribe sub-chondritic Pt:Pd ratios to the refractory behavior of Pt-alloys under conditions of dry melting associated with tholeiitic basalts; these phases are more fusible in the more fluid-rich melting regimes of metasomatized lithospheric mantle. Alternatively, Hughes et al. (2015) suggest that elevated (near-chondrite) Pt:Pd ratios in early magmas of the North Atlantic Igneous Province are the result of assimilation of fusible phases in previously Pt-enriched subcontinental lithospheric mantle. That the PGE-enriched rocks of the upper suite (e.g., picrites) have the same Pt:Pd ratio as the early, lower magmatic suite may suggest that these later magmas assimilated residual PGE-bearing phases from the lower magma conduit. Early segregation of a sulfide melt from the low TiO_2 magma could also explain the lack of PGE mineralization associated with this suite. The PGE endowment of the low TiO_2 phase may have been assimilated in the upper crust by the subsequent high TiO_2 magma.

DISCUSION AND CONCLUSIONS

Origin of the low TiO_2 and high TiO_2 Nikolai groups:

1) Trace-element composition points toward enriched MORB as a source for high TiO_2 Nikolai group
2) pMELTS modeling confirms the possibility of the high TiO_2 group being derived from a mantle source, however it cannot explain the low TiO_2 group sufficiently
3) Trace element modeling indicates that deep mantle partial melts mixing with Skolai Arc are required to produce the low TiO_2 Nikolai composition and can also explain the high TiO_2 Nikolai group
4) Elevated platinum group elements are associated with high TiO_2 ultramafic, high MgO olivine cumulates of the high TiO_2 Nikolai group.
5) The Pt/Pd composition of the high TiO_2 Nikolai group could suggest scavenging of the PGE from the low TiO_2 Nikolai by the ascending high TiO_2 Nikolai melts.

Two models have been proposed to explain the two groups within the Nikolai system. Greene et al. (2008) proposed a deep plume as the source of the volcanic rocks whereas Taylor et al. (2008) proposed decompressional melting of mantle due to intra- or back-arc rifting. Our geochemical modeling indicates the necessity of a depleted upper mantle component mixed with Skolai Arc to produce the low TiO_2 Nikolai member. The mixing with inherently heterogeneous arc could explain the scattered geochemical behavior of the low TiO_2 Nikolai samples. The tightness and homogeneity of the high TiO_2 Nikolai suggest that the homogeneous upper mantle was solely the source of those melts. The geochemical data could support both of the proposed models, however the geographic extent of the Nikolai groups following the arc suggests the back-arc/intra-arc spreading and decompressional melting is a more plausible scenario.

ACKNOWLEDGMENTS
This project is funded by the Legislature as part of the Governor's Strategic and Critical Minerals Assessment Capital Improvement Project which supplements the Airborne Geophysical/Geological Mineral Inventory as well as USGS National Cooperative Geologic Mapping Program STATEMAP component (award number G14AC00167 for 2014)

REFERENCES

DePaolo (1981). Trace element and isotopic effects of combined wallrock assimilation and fractional crystallization. Earth Planet. Sci. Letters, 53, 189–202.; Ghiorso, Hirschmann, Reiners, Kress, (2002). The pMELTS: A revision of MELTS for improved calculation of phase relations and major element partitioning related to partial melting of the mantle to 3 GPa. Geochem. Geophys. Geosyst., 3(5), 1–35.; Greene, Scoates, Weis, Israel, (2005). Flood basalts of the Wrangellia Terrane, southwest Yukon: Implications for the formation of oceanic plateaus, continental crust and Ni-Cu PGE mineralization. Yukon Explor. and Geol. 2004, 109–120.; Greene, A.R., Scoates, J.S., Weis, D., and Israel, S., 2005, Flood basalts of the Wrangellia Terrane, southwest Yukon: Implications for the formation of oceanic plateaus, continental crust and Ni-Cu PGE mineralization: Yukon Exploration and Geology 2004, p. 109-120.; Greene, Scoates, Weis, Nixon, Marsh, Carlson, Irvine, (2008). The Western Guichon Creek Complex: Insights into the Evolution of the Late Triassic Magmatism, Accretion and Metallogeny of Southern Stikinia, Yukon (Canada) segment of the accreted Wrangellia oceanic plateau. Lithos, 110(1-4), 1–19.; Hughes, McDonald, Arn (2015). Platinum-group element signatures in the North Atlantic Igneous Province: Implications for mantle controls on metal budgets during continental breakup. Lithos, 233, 89-110.; Manz, Barnes, (2004). Pt/Pd and Pd/Y ratios in mantle-derived magmas: A possible role for mantle metasomatism. S African J. Geol., 107, 333-340.; McDonough, Sun, (1995). The composition of the earth. Chem. Geol. 120, 223–253.; Pearce, (2008). Geochemical fingerprinting of oceanic basalts with applications to ophiolite classification and the search for Archean oceanic crust. Lithos, 100 (1), 14–48.; Pearce, Cann, (1973). Tectonic setting of basic volcanic rocks determined using trace element analyses. Earth Planet. Sci. Letters, 19 2, 290-300.; Nokleberg, Aleinikoff, Lange, Silva, Miyaoka, Schwab, Zehnerl, (1992). Preliminary geologic map of the Mount Hayes Quadrangle, eastern Alaska Range, Alaska. U.S. Dept. of the Interior, U.S.G.S. Open-File Report 92-594.; Taylor, Premo, Meier, Taggart, (2008). The metallogeny of Late Triassic rifting of the Alexander terrane in southeastern Alaska and northwestern British Columbia. Econ. Geol., 103, 89–115.; Twelker, Bachmann, Freeman, Newberry, Reioux, Sicard, Tuzzolino, Wright, Wypych, (2014). Major-Oxide, Minor-Oxide, and Trace-Element Geochemical Data from Rocks and Stream Sediments in the Wrangellia Mineral Assessment Area, Gulkana, Healy, Mount Hayes, and Talkeetna Mountains Quadrangles, Alaska. Div. of Geol. & Geoph. Surveys Raw-Data File 2014-3.; Workman, Hart, (2005). Major and trace element composition of the depleted MORB mantle (DMM). Earth Planet. Sci. Letters, 231(1-2), 53–72.; Wypych, Twelker, Freeman, Lande, Newberry, Reioux, Sicard, (2014). Major-Oxide and Trace-Element Geochemical Data from Rocks Collected in 2014 in the Wrangellia Mineral Assessment Area, Talkeetna Mountains C-4, C-5, and B-4 Quadrangles, Alaska. Div. of Geol. & Geoph. Surveys Raw-Data File 2014-22.; Wypych, Twelker, Freeman, Lande, Newberry, Reioux, Sicard, (2015). Major-Oxide and Trace-Element Geochemical Data From Rocks Collected in 2015 in the Wrangellia Mineral Assessment Area, Alaska. Div. of Geol. & Geoph. Surveys Raw-Data File 2015-16.